Explosive Boiling of Water Films Adjacent to Heated Surfaces: A Microscopic Description†

Yusheng Dou,‡,§ Leonid V. Zhigilei,‡,|| Nicholas Winograd,‡,§ and Barbara J. Garrison*,‡

Department of Chemistry and Materials Research Institute, Penn State University, University Park, Pennsylvania 16802, and Department of Materials Science and Engineering, University of Virginia, Charlottesville, Virginia 22903

Received: October 24, 2000; In Final Form: January 10, 2001

Molecular dynamics simulations are used to investigate the separation of water films adjacent to a hot metal surface. The simulations clearly show that the water layers nearest the surface overheat and undergo explosive boiling. For thick films, the expansion of the vaporized molecules near the surface forces the outer water layers to move away from the surface. These results are of interest for mass spectrometry of biological molecules, steam cleaning of surfaces, and medical procedures.

Introduction

Transparent fluids withdraw from a surface when an absorbing substrate is irradiated with an intense laser pulse. This phenomenon is central to a number of processes including eye surgery, selective killing of cells by irradiation of incorporated absorbing particles,[1] steam cleaning of surfaces,[2] and laser desorption mass spectrometry experiments of large biomolecules.[3−5] To understand the separation of a fluid from a laser-heated substrate, optical reflectance and scattering studies[6,7] as well as photoacoustic experiments[8] have been performed. These studies and others[3,5,9] suggest that a fast explosive phase transition occurs in the fluid adjacent to the irradiated surface.

The separation of the fluid from the absorbing particle is pictorially demonstrated in the high-speed imaging experiments of melanosomes irradiated by a 30 ps laser pulse.[10] In these experiments, the melanosomes that consist of absorbing pigment particles are embedded in a transparent liquid medium. Within 0.5 ns after the laser pulse, bubbles are visible only around the melanosomes and not within the liquid medium, indicating that the gas formation was localized adjacent to the surface of the absorbing particles. It was also noted that a threshold laser fluence was required to create the bubbles or film separation.

For laser desorption experiments, a biomolecule, e.g., DNA, is dissolved in water, deposited onto a metal substrate as a thin film, and frozen to 77 K.[3,4,5] The system is then irradiated with a laser pulse that goes through the transparent ice film and is absorbed by the substrate. The DNA molecule is desorbed intact directly into a mass spectrometer for molecular weight measurement. At this point, there are reproducibility problems with the experiment that appear to make it impractical for mass spectrometry.[4,5] These problems may arise from film thickness dependencies, metal surface chemistry issues, or concentration variations of the biomolecule. On the basis of the experimental protocol, steam cleaning of surfaces may have very similar physical processes occurring.

Despite suggestions in previous studies of the important physical processes involved, a detailed microscopic description of the events occurring at the interface between a fluid and a hot substrate is still lacking. In this paper, we present molecular dynamics (MD) simulations aimed at obtaining such a microscopic picture. Because of the importance of H_2O in many of the experiments, we have chosen it as our system. Water is also attractive as a system because of the extensive literature available on its physical properties. The interaction potentials available for MD simulations of H_2O are sufficiently reliable such that a quantitative analysis of the simulation results can be directly related to the thermodynamic parameters of water. From the variety of substrate materials used in different experiments, we have chosen to perform our first simulations using Au. This substance is chosen to match preliminary experiments with the selective killing of cells by inserted Au nanoparticles[11] and because of the availability of good interaction potentials for gold. In the simulations, we heat the Au substrate up to 1000 K. Calculations are performed for H_2O overlayers of different thickness. The motion of the H_2O overlayer, especially near the Au surface, is monitored pictorially and is explained in terms of the temperature gradients that develop in the film. The results show that the explosive boiling of the water film occurs near the surface and that the outward force from the phase transition separates the film from the metal creating a low-density region. We believe that the model presented here provides the basis for understanding of the molecular-level processes leading to the separation of a H_2O film from a heated substrate.

Methodology

The objective of the MD simulations[12] presented here is to model the microscopic motions in liquid films placed in contact with a hot surface. One essential component of MD simulations is the interaction potential from which the forces among the atoms and molecules are derived. Below we give our choices for the interaction potentials for the H_2O-H_2O, Au−Au, and $Au-H_2O$ components of the system. At the end of this section, the details of the MD simulations are described.

H_2O-H_2O Interaction. The potential employed to describe the H_2O-H_2O interaction is the simple-point-charge (SPC) water potential developed by Berendsen et al.[13] This potential has been used extensively to study the properties of H_2O as a solid,[14,15] liquid,[16−18] gas[19,20] and at the liquid/gas[21,22] interface. It has been shown that the SPC potential is able to reproduce

† Part of the special issue "William H. Miller Festschrift".
* To whom correspondence should be addressed.
‡ Department of Chemistry, Penn State University.
§ Materials Research Institute, Penn State University.
|| University of Virginia.

10.1021/jp003913o CCC: $20.00
Published on Web 02/08/2001

TABLE 1: Parameters of the Potential for the H_2O-H_2O and $Au-H_2O$ Interactions and the Molecular Geometry for SPC H_2O

H_2O-H_2O intermolecular potential parameters[16]	
q_{oxygen}	−0.82 e
$q_{hydrogen}$	+0.41 e
r_{off}	0.85 nm
σ	0.3166 nm
ϵ	6.7384×10^{-3} eV
H_2O molecular geometry	
$r_{equl.OH}$	0.10 nm
$\theta_{equl.HOH}$	109.47°
$Au-H_2O$ interaction parameters	
D_0	6.68×10^{-2} eV
β_0	13.0 nm^{-1}
β_H	13.0 nm^{-1}
r_{e1}	0.37 nm
r_{e2}	−0.10 nm
γ	0.2

many of the properties of bulk[16] H_2O and the liquid/vapor interface[22] of H_2O. In the SPC model, the molecular interaction potential U_{inter} consists of an electrostatic component $U_{electrostatic}$ describing the charge−charge interaction between pairs of atoms in the two molecules. In order to describe the dispersion and repulsive interactions between the two oxygen sites, a Lennard-Jones function U_{LJ} is included. The total interaction potential between molecules i and j is given as

$$U_{inter} = U_{LJ} + U_{electrostatic} = 4\epsilon\left[\left(\frac{\sigma}{r_{ij}}\right)^{12} - \left(\frac{\sigma}{r_{ij}}\right)^{6}\right] + \sum_{l=1}^{3}\sum_{k=1}^{3}\frac{q_{ik}q_{jl}}{(4\pi\epsilon_0 r_{kl})} \quad (1)$$

where r_{ij} is the distance between oxygen atoms and the summation runs over the partial charges k and l of the molecules. All parameters in eq 1 are listed in Table 1.

The electrostatic term in eq 1 requires special care in the simulations because it is long-ranged and, typically, MD simulations use periodic boundary conditions in which only particles within a given cutoff distance are included in the force calculation. One approach for including all of the electrostatic interactions is to use an Ewald summation.[12] The violent motion that occurs in the simulations presented here, however, makes the Ewald prescription challenging. Another approach for handling the electrostatic interaction is to switch it off at a distance r_{off}.[23−25] There are a number of switching approaches including smoothly switching off the potential or/and the force. We have chosen to modify the electrostatic potential by a force shifting approach.[24] In this method, the electrostatic term is modified by a force shifting function $S_1(r)$ as

$$U'_{electrostatic} = S_1(r)\, U_{electrostatic} \quad (2)$$

where the force shifting function is given by

$$S_1(r) = \begin{cases} \left(1 - \dfrac{r}{r_{off}}\right)^2 & r < r_{off} \\ 0 & r \geq r_{off} \end{cases} \quad (3)$$

The force shifted potential $U'_{electrostatic}$ yields a smooth variation in the electrostatic interaction force by shifting the force from the true Coulombic force by a constant. Because of the absence of discontinuities in the force, this scheme results in smaller fluctuations in the total energy during the MD simulation than other truncation schemes, such as the spherical cutoff method and the switch potential method.[24] The force-shifted potential significantly alters the individual short-range interactions of charged atoms because it modifies the potential at all distances. The electrostatic interactions in water, however, are used to create a net dipole−dipole interaction by near cancellation of repulsive and attractive ionic terms. Consequently, the corrections due to shifting the force tend to be canceled. Using an integral equation method, Brooks et al. have shown that the force shift potential is able to reproduce more accurately the short-range structure of H_2O than the shifted potential.[23] More recently, Prevost et al. calculated the structural and dynamical properties of liquid water using the shifted and force shifted potentials and compared the results with those obtained using an Ewald summation.[25] They found that the radial pair distribution functions, the mean potential energy, and the diffusion coefficient calculated are closer to the Ewald results using the force shifted potential than using the shifted potential.

Au−Au Interaction. The Au−Au interactions are represented by the MD/Monte Carlo corrected effective medium (MD/MC−CEM) potential function for fcc metals.[26] This potential has been fit to bulk properties of Au as well as to the low coordination configuration of Au_2. Most importantly, it reasonably reproduces the experimental surface energy of Au.[27] The potential function has been used in MD studies of thermal properties of alkanethiolate overlayers on a Au surface[28] as well as molecular ejection induced by keV particle bombardment of benzene,[29] polystyrene oligomers,[30] and alkanethiolates[31] adsorbed on a Au(111) surface.

Au−H_2O Interaction. An interaction potential for metal−water systems has been developed by Spohr[32] and used in a number of studies investigating H_2O adsorption on Ni(100)[32] and Pt(111)[33] surfaces. The Spohr function consists of a Morse function combined with a corrugation term defining various surface sites for the oxygen-surface interaction and a repulsive term for the hydrogen-surface interaction. An inherent assumption in this potential is that the metal surface is rigid. Because we need the metal atoms to move and interact with the water molecules, we have modified the Spohr function so that the interactions are pairwise additive between the O and H atoms in the H_2O molecule and the metal atoms. Our modified potential has the form

$$U_{M-H_2O} = U_{M-O}(r_{M-O}) + U_{M-H1}(r_{M-H1}) + U_{M-H2}(r_{M-H2}) \quad (4)$$

with

$$U_{M-O}(r) = D_0[\exp(-2\beta_0(r - r_{e1})) - 2\exp(-\beta_0(r - r_{e1}))] \quad (5)$$

and

$$U_{M-H}(r) = \gamma D_0 \exp(-2\beta_H(r - r_{e2})) \quad (6)$$

In the Spohr function, the value of D_0 is adjusted to give an adsorption energy of 10.5 kcal/mol as determined from thermal programmed desorption experiments.[34] The values of r_{e1} are chosen to give the experimental distance of the water molecule from the surface.[35] The values of β are chosen to give the same curvature and range as the original Spohr function. The values for all parameters in eqs 5 and 6 are listed in Table 1.

For computational efficiency it is necessary to cutoff the M−O and M−H interactions. The M−H interaction rapidly approaches zero given the choice of parameters in Table 1. It is thus merely truncated at 6 Å. The potential function $U_{M-O}(r)$ is switched to zero at a longer distance

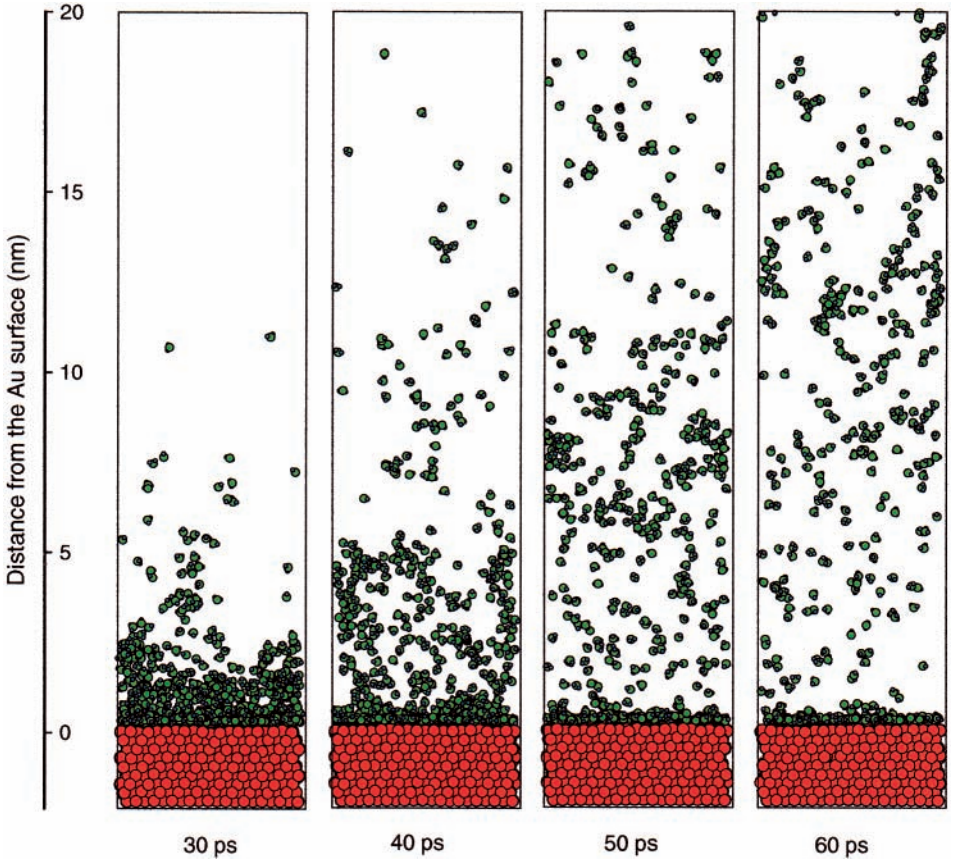

Figure 1. Snapshots from the MD simulation of six water layers on a Au(111) surface heated to 1000 K. The green, blue, and red spheres represent oxygen, hydrogen and gold atoms, respectively. The time between successive frames is 10 ps.

$$U_{M-O} = S_2(r)\, U_{M-O}(r) \tag{7}$$

The switch function S_2 has the form[24]

$$S_2(r) = \begin{cases} 1 & r \le r_{on} \\ \dfrac{(r_{off}^2 - r^2)^2(r_{off}^2 + 2r^2 - 3r_{on}^2)}{(r_{off}^2 - r_{on}^2)^3} & r_{on} < r \le r_{off} \end{cases} \tag{8}$$

where r_{on} and r_{off} are the start and end distances of switch function and are set to 7.0 and 11.0 Å, respectively.

Systems and MD Simulation. MD simulations have been performed for three systems. A face centered cubic crystallite composed of 1980 Au atoms arranged in nine (111) layers of 220 atoms each is used in all of the simulations. Periodic boundary conditions in the directions parallel to the surface are imposed. Three systems containing 6 layers (528 molecules), 12 layers (1056 molecules), and 24 layers (2112 molecules) are investigated. Initial H_2O films are constructed based on a hexagonal arrangement of O atoms as in the Ih ice structure. The H_2O molecules in the first layer, just above the Au(111) surface, are oriented so that the angles between the surface normal and both OH bonds are about 109°. The H_2O molecules in the second layer are arranged as if each molecule has one H atom oriented to form a hydrogen bond with the O atom in the first layer and one H atom oriented to form a hydrogen bond with the O atom in the third layer. The water molecules in subsequent pairs of layers repeat the orientation patterns of those in the first and second layers.

The equations of motion are integrated using the velocity Verlet algorithm[36] in conjunction with the RATTLE constraint method[37] to maintain fixed O−H bond lengths and a fixed H−O−H bond angle.[38] On the basis of energy conservation tests, a time step of 1.0 fs is chosen.

To induce film separation, the Au surface must be quickly heated. As a first step, we have chosen to use a nearly instantaneous temperature increase in the metal substrate. A value of 1000 K is chosen for the temperature because it ensures we are above the fluence threshold as observed in bubble formation,[10] it is well above the critical temperature of H_2O and it is below the melting temperature of Au. Because the rate of heating and the final temperature can be important, we are investigating the influence of these parameters on the film separation process.[39]

The Au substrate is heated according to the following protocol. The Au atoms at the bottom layer are kept rigid in order to prevent small migrations of the sample. In addition to the forces from the MD/MC−CEM interactions, the atoms located in the next four layers are subjected to friction and stochastic forces as prescribed by the Generalized Langevin equation method.[40] The temperature of the stochastic region is maintained at 1000 K. The top four Au layers equilibrate with the stochastic region within about 3 ps. The entire Au substrate is maintained at 1000 K throughout the simulation.

Results and Discussions

In this section, we present the simulation results for H_2O overlayers on a Au (111) surface heated to 1000 K. These results provide insight into the elementary processes involved in the fast phase transformations in the water layer adjacent to the substrate. First, we present a qualitative visual analysis of the microscopic motions in the H_2O film. The temperature evolution in the system is then discussed.

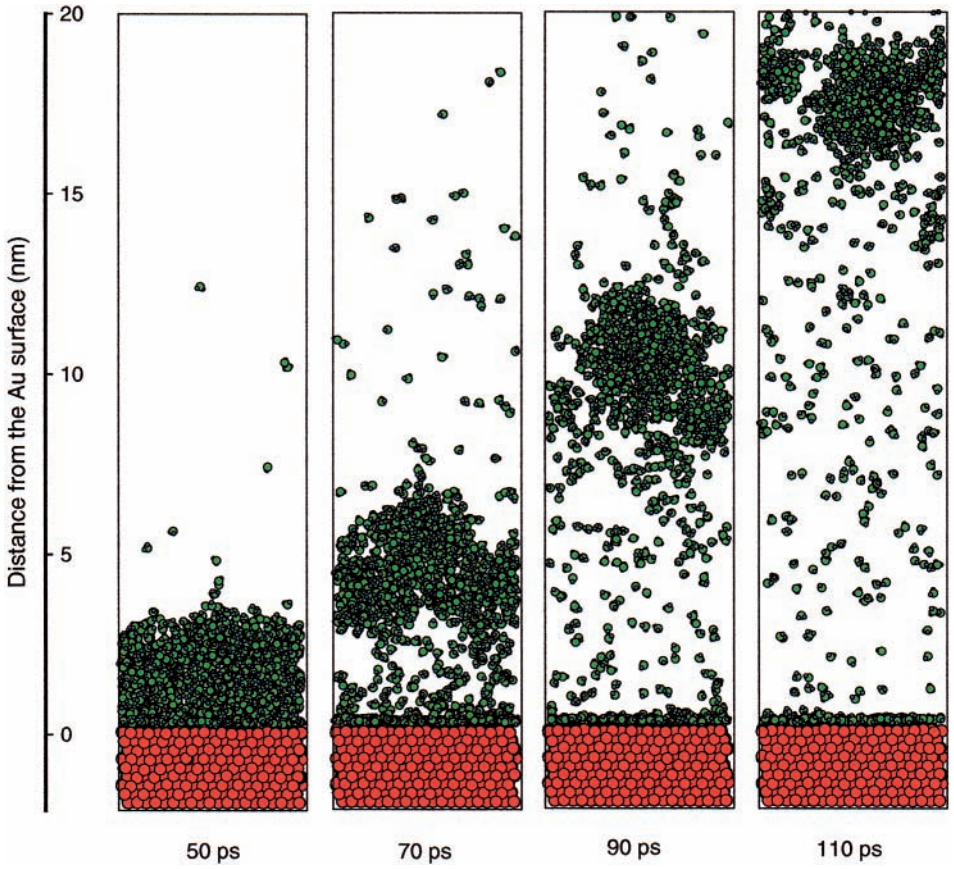

Figure 2. Snapshots from the MD simulation of 12 water layers on a Au(111) surface heated to 1000 K. The time between successive frames is 20 ps.

Snapshots at different times during the simulations are shown in Figures 1−3. For the 6-layer system (Figure 1), the top approximately 4−5 layers vaporize from the surface in the form of individual molecules and very small clusters. The H_2O molecules that remain near the surface at 60 ps will also eventually desorb by about 250 ps. For the 12-layer system (Figure 2) and the 24-layer system (Figure 3), the H_2O molecules near the surface vaporize and push large aggregates of H_2O molecules away from the surface, a scenario that could be relevant to the bubble formation around laser irradiated melanosomes.[10]

The physics of the process observed in Figures 1−3 can be clarified by examining the temperature evolution within the H_2O film during the course of the simulation. Contour plots showing the temperature for the three systems as a function of time and distance from the top Au layer are shown in Figure 4. The temperature is defined by using only the radial component of the kinetic energy as in simulations of laser ablation.[41] The temperatures for phase transitions of H_2O at 1 atm are 273 K (melting), 373 K (boiling), and about 500 K (explosive boiling[42]). The corresponding color regimes in Figure 4 are teal for melting, green for boiling, and the pink/orange interface for explosive boiling. The temperature evolution for the six-layer system (Figure 4a) shows that the entire film attains a temperature over 500 K within approximately 20 ps. Consequently, the entire film vaporizes within the next few tens of picoseconds. For the thicker films, the thermal conductivity in the H_2O film is sufficiently slow so that a temperature gradient is established. At around 35 ps in the 12-layer system, the water molecules located near the surface reach the temperature for explosive boiling (orange/pink boundary), whereas the top of the film is only at the boiling temperature (Figure 4b). The effect of the phase explosion in the lower layers is to provide the acceleration for moving the molecules in the top layers outward from the surface (Figure 2). The temperature gradient is even more pronounced for the 24-layer system shown in Figure 4c. At approximately 50 ps the water layers near the surface approach the temperature for explosive boiling, whereas the top of the film is now only in the melting regime.

Explosive boiling, or a phase explosion, occurs when thermal energy is deposited too fast for normal boiling to happen.[43,44,45] Consequently, the material overheats to the limit of it thermodynamic stability, a value close to the critical temperature. It has been predicted from thermodynamic arguments that the phase transformation in this case proceeds in an explosive manner leading to a rapid decomposition of the overheated region into gas phase molecules and liquid droplets. The relevance of the phase explosion has been discussed for a number of phenomena in which a sufficiently fast heating can be realized, such as short pulse laser irradiation,[43,46,47] ion bombardment,[45] or pulsed electrical heating of a conducting wire.[48] A pictorial molecular-level view of the phase explosion has been provided by recent MD simulations of laser ablation.[49,50] In the simulations presented here, the transfer of thermal energy from a hot metal substrate is shown to be sufficiently fast to overheat a thin layer of water adjacent to the metal surface well past the normal boiling point and to provide the conditions for phase explosion. In the case of the 6-layer system, the entire film of H_2O molecules is overheated and all molecules are ejected. For the 12- and 24-layers systems, the explosive boiling occurs only in a region close to the heated substrate and generates the outward force for moving the upper part of the water overlayer away from the substrate. As a result, a low-density region is formed between the substrate and the top part

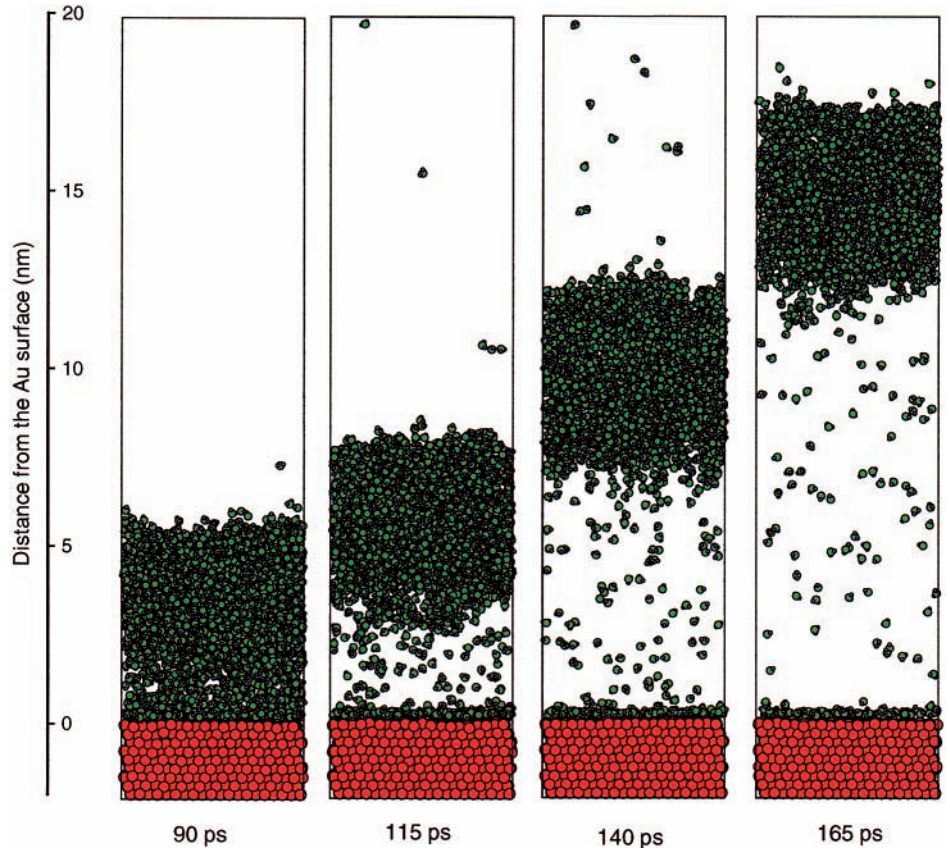

Figure 3. Snapshots from the MD simulation of 24 water layers on a Au(111) surface heated to 1000 K. The time between successive frames is 25 ps.

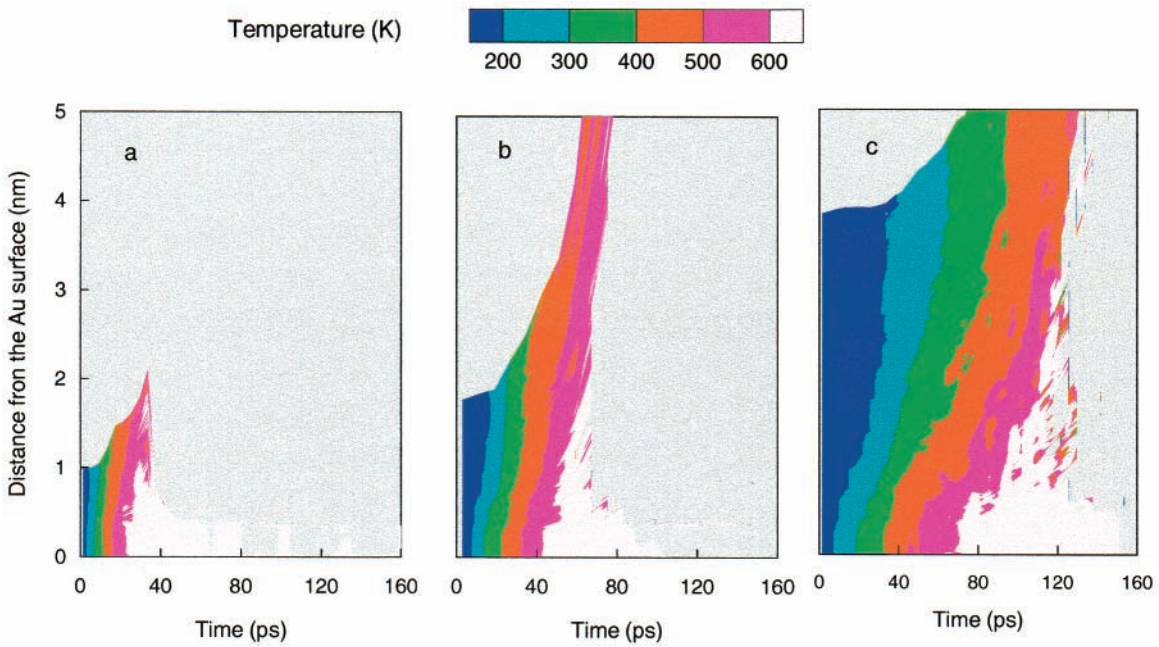

Figure 4. Temperature contour plots of the H_2O phase as a function of time and distance from the top Au layer. (a) 6-layer system, (b) 12-layer system, (c) 24-layer system.

of the water overlayer and the energy transfer from the metal surface is interrupted. In the 24-layer system, the top part of the overlayer ejects with a temperature above the boiling point but below the temperature needed for the phase explosion. The upward moving layer is cooled by intensive evaporation and is disintegrated into liquid droplets, as observed later in the 12-layer system. In the present simulations as well as in simulations performed for thicker H_2O overlayers[51] we find that both the average temperature of the ejected layer and the ejection velocity decrease as the thickness of the overlayer increases. Simulations with thick overlayers can be related to recent experimental observation of overlayers that "jump" as a result of the energy deposition into the metal substrate by a short pulse laser irradiation.[9] In the limit of an infinitely thick overlayer, the outward force from the phase explosion would result in a compressive pressure wave propagating through the medium

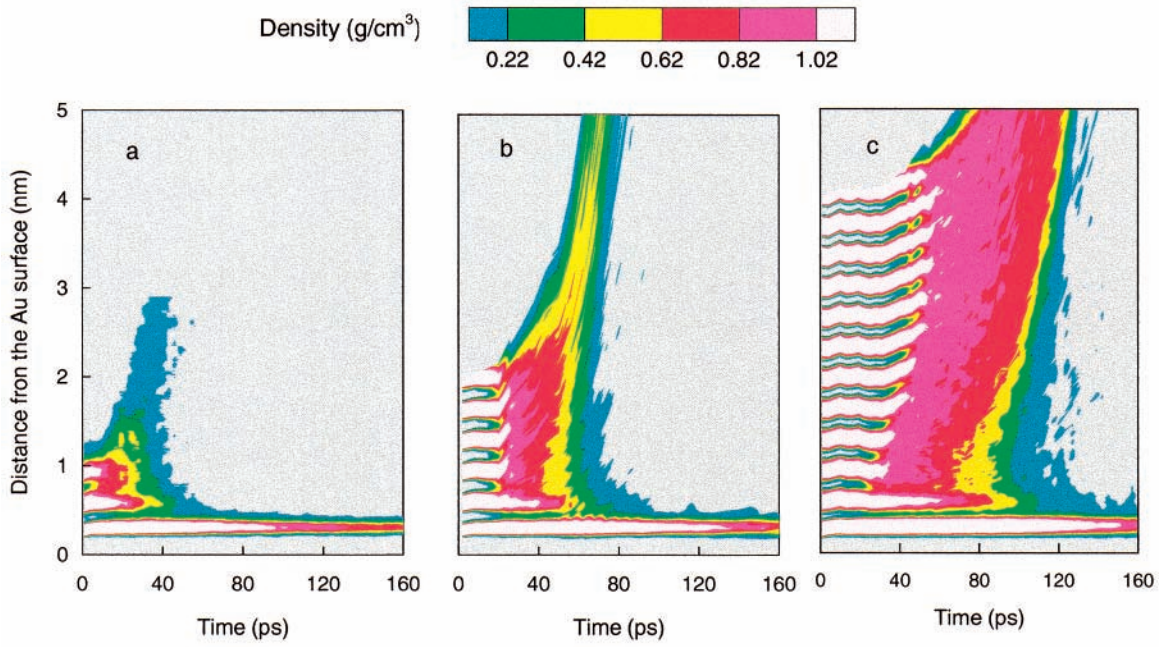

Figure 5. Density contour plots of the H_2O phase as a function of time and distance from the top Au layer. (a) 6-layer system, (b) 12-layer system, (c) 24-layer system.

as observed in the experiments of the melanosomes in the transparent medium.[10]

Complementary information on the film dynamics can be obtained from density contour plots shown in Figure 5. In the initial structure of the water film, there are pairs of layers in which the O atoms have approximately the same height above the metal surface. Consequently, only three, six, and 12 white bands of density greater than 1 g/cm^3 are observed in Figure 5 for the 6-, 12-, and 24-layer systems, respectively. For all systems, the two layers of H_2O molecules closest to the Au remain on the surface the longest because the binding energy to the surface in our computational system is greater than the cohesive energy of the water film. In the discussion below, this group of H_2O molecules is ignored. For the 6-layer system (Figure 5a), the density is higher near the surface and lower near the vacuum for times after 10−20 ps. Moreover, the disappearance of the crystalline order (high density regions shown as white contours) occurs first for the upper layer. At the other extreme, for the 24-layer system (Figure 5c), a density inversion occurs. The loss of the crystalline order occurs first near the surface at approximately 35 and 20 ps later at the top of the film reflecting the temperature gradient in the film as shown in Figure 4c.

The time development of the average temperature of all H_2O molecules is shown in Figure 6. When the results for the 6-layer system were examined first, the temperature of the overlayer rises until about 40 ps. As can be observed from Figure 1, the molecules are for the most part vaporized. Consistent with the physics of a phase transition, the film cools. The heating of larger 12-layer and 24-layer systems takes longer time, and the maximum average temperatures are lower.

There are possible implications of these results for both mass spectrometry with the water matrix and the bubble formation around absorbing particles. In the mass spectrometry experiments, the objective is to get the entire analyte molecule off of the surface without decomposing it and free of water molecules. From the animation snapshots in Figures 1−3, the best conditions appear to be for the 6-layer film where most of the ejection of the material occurs as individual molecules. From

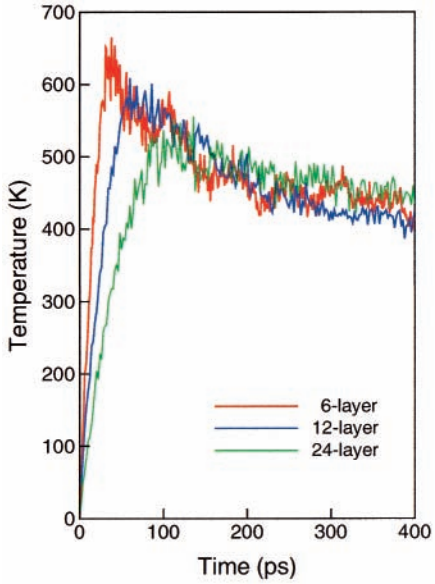

Figure 6. Radial kinetic energy vs time for the three systems.

the heating curve in Figure 6, however, the thin layer appears to be the hottest. On the other hand, the thin layer rapidly cools, thus there is the possibility that the analyte molecule will not be overheated. The aggregate of molecules moving upward in the 24-layer system still has a temperature well above the boiling point as shown in Figure 4c at ~150 ps. This aggregate will cool by an intensive vaporization, a slower cooling process than the explosive boiling.[46] Analyte molecules in this part of the H_2O film may become rather hot. This scenario of the thin H_2O layers being the best environment for the analyte molecule is consistent with the observed rim effect in which the best MALDI spectra occurred when taken near the edge of the ice crystals rather than in the thicker center part.[5] Although we have predicted the temperature changes in the H_2O layer, there is a question of whether an incorporated analyte molecule will equilibrate with the matrix. Recent atomistic MD simulations[52] indicate that the energy transfer from the matrix molecules to

the analyte molecule could be limited by a bottleneck in the energy transfer[53] because of the weak coupling between the internal high-frequency vibrational modes of analyte molecules and the motions of the matrix molecules.

The pictorial results of Figures 2 and 3 are reminiscent of the bubbles formed around the laser-irradiated melanosomes.[10] The full implications of the heat transfer along with the outgoing pressure wave will be investigated in simulations that maintain the external pressure and allow for the outward flow of energy.

Summary

In this work, we have developed the initial framework for a MD model that describes the dynamics of the vaporization of a H_2O film adjacent to a laser-irradiated metal surface. The simulation results show that the H_2O molecules are overheated and undergo an explosive boiling. The H_2O film is found to completely desorb from the surface. The temperature and structure of the desorbed layer, however, are strongly dependent upon its thickness. This dependency appears because the region of the film associated with the phase explosion is restricted to the few layers in contact with the metal. The outward force generated by the explosion separates the water film from the metal surface, creating a low-density region. These MD results are in qualitative agreement with observations in several experiments.

Although the model presented here is clearly in its initial stages, we believe that it represents a first step in identifying the important parameters that influence explosive boiling at heated substrates. One of these parameters is the optimal H_2O thickness for the embedded molecules to be desorbed without overheating or over-solvation in the case of mass spectrometry experiments. Other interesting questions that arises in both the mass spectrometry experiments and steam cleaning of surfaces are (i) how will incorporation of an embedded molecule influence the dynamics of desorption and (ii) how much water needs to be around a contaminant particle to lift it off. For the case of absorbing particles such as melanosomes, the impact of an outward pressure wave needs to be assessed in conjunction with the observation of irreversible damage to the cell.

The simulations presented here and in recent studies of laser ablation[49,50] clearly demonstrate that explosive boiling can occur in a relatively short time. There are open questions about the microscopic nature of explosive boiling and its dependence on the time scale of the heating process.[44,46,47] Studies are underway to address these questions.[54]

Acknowledgment. The financial support of the Office of Naval Research through the Medical Free Electron Program, the National Science Foundation, the National Institute of Health, and the IBM Selected University Research Program are gratefully acknowledged. The Center for Academic Computing at Penn State University provided computational assistance. We thank Antonio Miotello for insightful discussion and suggestions and Tatiana Itina for suggestions on the manuscript.

References and Notes

(1) Lin, C. P.; Kelly, M. W.; Sibayan, S. A. B.; Latina, M. A.; Anderson, R. R. *IEEE J. Sel. Top. Quantum Electron.* **1999**, *5*, 963.

(2) See, for example, Tam, A. C.; Leung, W. P.; Zapka, W.; Ziemlich, W. *J. Appl. Phys*. **1992**, *71*, 3515. She, M.; Kim, D.; Grigoropoulos, C. P. *J. Appl. Phys.* **1999**, *86*, 6519. Lu, Y. F.; Song, W. D.; Zhang, Y.; Low, T. S. *Proc. SPIE Int. Soc. Opt. Eng.* **1998**, *3550*, 7.

(3) Nelson, R. W.; Rainbow, M. J.; Lohr, D. E.; Williams, P. *Science* **1989**, *246*, 1585. Nelson, R. W.; Thomas, R. M.; Williams, P. *Rapid Commun. Mass Spectrom.* **1990**, *4*, 349. Williams, P.; Nelson, R. W. In *Methods and Mechanisms for Producing Ions from large Molecules*, *NATO ASI Series* 269; Standing, K. G., Ens, W., Eds.; Plenum Press: New York, 1991; p 265.

(4) Schieltz, D. M.; Chou, C.-W.; Luo, C.-W.; Thomas, R. M.; Williams, P. *Rapid Commun. Mass Spectrom.* **1992**, *6*, 631.

(5) Williams, P. *Int. J. Mass Spectrom. Ion. Processes* **1994**, *131*, 335.

(6) Yavas, O.; Leiderer, P.; Park, H. K.; Grigoropoulos, C. P.; Poon, C. C.; Leung, W. P.; Do, N.; Tam, A. C. *Phys. Rev. Lett.* **1993**, *70*, 1830.

(7) Park, H. K.; Grigoropoulos, C. P.; Poon, C. C.; Tam, A. C. *Appl. Phys. Lett*. **1996**, *68*, 596.

(8) Park, H. K.; Kim, D.; Grigoropoulos, C. P.; Tam, A. C. *J. Appl. Phys*. **1996**, *80*, 4072.

(9) Talrose, V. L.; Person, M. D.; Whittal, R. M.; Walls, F. C.; Burlingame, A. L.; Baldwin, M. A. *Rapid Commun. Mass Spectrom.* **1999**, *13*, 2191.

(10) Lin, C. P.; Kelly, M. W. *Appl. Phys. Lett*. **1998**, *72*, 2800.

(11) Lin, C. P. Personal communication.

(12) Allen, M. P.; Tildesley, D. J. *Computer Simulation of Liquids*; Oxford Press: New York, 1994.

(13) Berendsen, H. J. C.; Postma, J. P. M.; van Gunsteren, W. F.; Hermans, J. in *Intermolecular Forces*; Pullman, B., Ed.; Reidel: Dordrecht, The Netherlands, 1981.

(14) Impey, R. W.; Klein, M. L.; Tse, J. S. *J. Chem. Phys*. **1984**, *81*, 8406.

(15) Lombardero, M.; Martin, C.; Jorge, S.; Lado, F.; Lomba, E. *J. Chem. Phys*. **1999**, *110*, 1148.

(16) Wallqvist, A.; Teleman, O. *Mol. Phys*. **1991**, *74*, 515.

(17) Toukan, K.; Rahman, A. *Phys. Rev. B* **1985**, *31*, 2643.

(18) Barrat, J.-L.; McDonald, I. R. *Mol. Phys*. **1990**, *70*, 535.

(19) Marti, J.; Padro, J. A.; Guardia, E. *Mol. Phys*. **1995**, *86*, 263.

(20) Padro, J. A.; Marti, J.; Guardia, E. *J. Phys. Condens. Matter*. **1994**, *6*, 2283.

(21) Guissani, Y.; Huillot, B. *J. Chem. Phys*. **1993**, *98*, 8221.

(22) Taylor, R. S.; Dang, L. X.; Garrett, B. C. *J. Phys. Chem*. **1996**, *100*, 11720.

(23) Brooks, C. L. III; Pettitt, B. M.; Karplus, M. *J. Chem. Phys*. **1985**, *83*, 5897.

(24) Steinbach, P. J.; Brooks, B. R. *J. Comput. Chem*. **1994**, *15*, 667.

(25) Prevost, M.; van Belle, D.; Lippens, G.; Wodak, S. *Mol. Phys*. **1990**, *71*, 587.

(26) Stave, M. S.; Sanders, D. S.; Raeker, T. J.; DePristo, A. E. *J. Chem. Phys*. **1990**, *93*, 4413. Raeker, T. J.; DePristo, A. E. *Int. Rev. Phys. Chem.* **1991**, *10*, 1. Kelchner, C. L.; Halstead, D. M.; Perkins, L. S.; Wallace, N. M. *Surf. Sci*. **1994**, *310*, 425.

(27) DePristo, A. E. In *Recent Advances in Density Functional Theory: Part 2 Methodology*; Chong, D., Ed.; World Scientific: River Edge, N.J., 1995.

(28) Mahaffy, R. E.; Bhatia, R.; Garrison, B. J. *J. Phys. Chem. B* **1997**, *101*, 771. Bhatia, R.; Garrison, B. J. *Langmuir* **1997**, *13*, 765; **1997**, *13*, 4038.

(29) Chatterjee, R.; Postawa, Z.; Winograd, N.; Garrison, B. J. *J. Phys. Chem. B* **1999**, *103*, 151.

(30) Delcorte, A.; Eynde, X. V.; Bertrand, P.; Vickerman, J. C.; Garrison, B. J. *J. Phys. Chem. B* **2000**, *104*, 2673.

(31) Liu, K. S. S.; Yong, C. W.; Garrison, B. J.; Vickerman, J. C. *J. Phys. Chem. B* **1999**, *103*, 3195.

(32) Spohr, E. *J. Mol. Liq*. **1995**, *64*, 91.

(33) Spohr, E. *J. Electroanal. Chem*. **1998**, *450*, 327.

(34) Kay, B. D.; Lykke, K. R.; Creighton, J. R.; Ward, S. J. *J. Chem. Phys*. **1989**, *91*, 5120.

(35) Thiel, P. A.; Madey, T. E. *Surf. Sci. Rep.* **1987**, *7*, 211 and references therein.

(36) Swope, W. C.; Anderson, H. C.; Berens, P. H.; Wilson, K. R. *J. Chem. Phys*. **1982**, *76*, 637.

(37) Andersen, H. C. *J. Comput. Phys*. **1983**, *52*, 24.

(38) The vibrational partition functions for the two stretch modes of H_2O at 600 K are only 0.01% greater than unity. The partition of the bending mode is 1.02 at 600 K. Thus no significant amount of heat should flow into these modes at the temperatures of interest in this study.

(39) Dou, Y.; Zhigilei, L. V.; Winograd, N.; Garrison, B. J. Work in progress.

(40) Garrison, B. J.; Kodali, P. B. S.; Srivastava, D. *Chem. Rev*. **1996**, *96*, 1327 and references therein.

(41) Zhigilei, L. V.; Garrison, B. J. *Appl. Phys. Lett.* **1997**, *71*, 551; *Rapid Commun. Mass Spectrom.* **1998**, *12*, 1273.

(42) The temperature value for explosive boiling is estimated as 0.8 the critical temperature which is 640 K at 1 atm. Avedisian, C. T. *J. Phys. Chem. Ref. Data* **1985**, *14*, 695.

(43) Martynyuk, M. M. *Sov. Phys. Technol. Phys.* **1976**, *21*, 430.

(44) Kelly, R.; Miotello, A. *Appl. Surf. Sci.* **1996**, *96*, 205.

(45) Sunner, J.; Ikonomou, M. G.; Kebarle, P. *Int. J. Mass Spectrom. Ion Processes* **1988**, *82*, 221.

(46) Miotello, A.; Kelly, R. *Appl. Phys. A* **1999**, *69*, S67.

(47) Kelly, R.; Miotello, A. *Phys. Rev. E* **1999**, *60*, 2616.
(48) Martynyuk, M. M. *Sov. Phys. Technol. Phys.* **1974**, *19*, 793.
(49) Zhigilei, L. V.; Kodali, P. B. S.; Garrison, B. J. *J. Phys. Chem. B* **1997**, *101*, 2028; *J. Phys. Chem. B.* **1998**, *102*, 2845; *Chem. Phys. Lett.* **1997**, *276*, 269.
(50) Zhigilei, L. V.; Garrison, B. J. *J. Appl. Phys.* **2000**, *88*, 1281; *Appl. Phys. Lett.* **1999**, *74*, 1342.
(51) Dou, Y.; Zhigilei, L. V.; Postawa, Z.; Winograd, N.; Garrison, B. J. *Nucl. Instr. Methods B*, in press.
(52) Bencsura, A.; Navale, V.; Sadeghi, M.; Vertes, A. *Rapid Commun. Mass Spectrom.* **1997**, *11*, 679.
(53) Vertes, A.; Gijbels, R.; Levine, R. D. *Rapid Commun. Mass Spectrom.* **1990**, *4*, 228.
(54) Itina, T. E.; Zhigilei, L. V.; Garrison, B. J. Personal communication.